Response of microchannel plates to single particles and to electromagnetic showers

F. Cavallari [b], D. Del Re [b], S. Gelli [b], A. Ghezzi [a], C. Gotti [a], P. Govoni [a], C. Jorda [b], A. Martelli [a], B. Marzocchi [a], P. Meridiani [b], G. Organtini [b], R. Paramatti [b], S. Pigazzini [a], S. Rahatlou [b], C. Rovelli [b], F. Santanastasio [b], T. Tabarelli de Fatis [a,*], N. Trevisani [a]

[a] *Università di Milano Bicocca and INFN, Sezione di Milano-Bicocca, Piazza della Scienza 3, I-20126, Milano, Italy*

[b] *Sapienza Università di Roma and INFN, Sezione di Roma1, P.le A. Moro 1, I-00044 Rome, Italy*

Abstract

We report on the response of microchannel plates (MCPs) to single relativistic particles and to electromagnetic showers. Particle detection by means of secondary emission of electrons at the MCP surface has long been proposed and is used extensively in ion time-of-flight mass spectrometers. What has not been investigated in depth is their use to detect the ionizing component of showers. The time resolution of MCPs exceeds anything that has been previously used in calorimeters and, if exploited effectively, could aid in the event reconstruction at high luminosity colliders. Several prototypes of photodetectors with the amplification stage based on MCPs were exposed to cosmic rays and to 491 MeV electrons at the INFN-LNF Beam-Test Facility. The time resolution and the efficiency of the MCPs are measured as a function of the particle multiplicity, and the results used to model the response to high-energy showers.

Key words: Micro-channel plates, secondary emission, electromagnetic showers, time response, calorimetry
PACS: xx.yy.zz, xx.yy.zz

* Corresponding author: tommaso.tabarelli@mib.infn.it

1 Introduction

With the packet structure of beams at hadron colliders, high luminosities are achieved at the cost of an increased number of concurrent collisions per beam crossing at the experiment collision point. At the LHC, there are typically 20-30 overlapping interactions per beam crossing, spread over a length of about 5 cm root mean square (RMS) along the beam axis. Event reconstruction exploits the association of individual particles to an interaction vertex: tracks or energy deposits inconsistent with the vertex of interest are filtered, or statistically subtracted. This approach becomes strained at the High-Luminosity LHC (HL-LHC) - and, in prospect, at future colliders -, where about 140-200 collisions per beam crossing are anticipated. With peak vertex densities above 1 mm^{-1}, tracks from nearby vertices could be merged into a fake, high-energy event vertex [1]. More importantly, even at moderate vertex densities, the random overlap of energy deposits from neutral particles - mainly photons -, which cannot be tied to any vertex, deteriorates the performance of calorimeters in terms of energy measurement and particle identification, as particles appear to be less isolated. A precise measurement of the time of the energy deposits, and of each collision vertex has been advocated as a means to mitigate these effects [2]. Due to the length of the packets, collision vertices at the HL-LHC have a time spread of about 200 ps RMS. A time resolution of about 20 ps would therefore reduce the 'effective multiplicity' of concurrent collisions by a factor 10, down to a level comparable to the LHC. This resolution is one order of magnitude better than at current LHC experiments [3], [4], [5].

In this work, we characterize the response of microchannel plates (MCPs) [6] to single relativistic particles and to the ionizing component of electromagnetic showers. Due to their superior time response, a layer of MCPs embedded in a calorimeter, or in a preshower compartment of it, could be exploited to provide a precise measurement of the photon time. In addition, even for moderate efficiencies to minimum ionizing particles, the time of each vertex could be reconstructed from the time of energy deposits associated to charged tracks, owing to the large track multiplicity at hadron colliders. This detector would therefore enable, at once, time separation of vertices in spatial overlap and assignment of the neutral energy to the proper vertex. A preshower would factorize the quest for precision timing from the technological choice of the full calorimeter in future experiments, or could be added in front of existing calorimeters in an upgrade program of current detectors.

The use of secondary emission of electrons at the MCP surface to sample the ionizing component of showers was pioneered in 1990 [7]. The MCP response to relativistic particles was also investigated in the '90s, and detection efficiencies of around 70%, with time resolution of 70 ps were achieved [8]. Recent technological progress of the Large Area Picosecond Photodetector Collabo-

ration [9] may result in a reduction of the cost production for MCPs and is spurring a renewed interest in this detection techniques. A set of measurements - similar in scope to our work - has been recently reported in [10], where the response of photodetectors based on MCP multipliers was tested in proton and positron beams. Time resolution of order 20-30 ps at shower maximum were obtained. The contribution to the detector response from secondary emission at the MCP surface was indirectly inferred by estimating the contribution from Cherenkov emission in the optical window of the photodetector at different window thicknesses.

At variance with that work, we directly measure and characterize the secondary emission from the MCP surface in MCP-based photomultipliers (PMT-MCP), by applying a retarding bias to the photocathode, in order to inhibit avalanche formation from electrons emitted at the photocathode. We refer to this setup as to an 'ionization-MCP' (i-MCP). Measurements are also reported for the PMT-MCP operation mode, where Cherenkov emission from the photodetector window was exploited. The potential advantage of an i-MCP consists in the elimination of the photocathode, resulting in a more robust design and in a potentially improved radiation tolerance, since radiation damage mostly affects the photocathode response [11].

In this paper, after the description of the detectors and of the measurement setup (Sec. 2), we present results on the response to single particles and to showers at different depths in radiation lengths (Sec. 3 and 4). A response model for the MCPs is developed along with the discussion of the results, and then used to anticipate the performance of a preshower detector (Sec. 5). Ways to further improve the response of i-MCPs are also indicated.

2 Detector description and operation modes

Our measurements are carried out with PMT-MCPs developed at BINP (Novosibirsk), in collaboration with the Ekran FEP manufacturer. Full characterization of these photodetectors is reported in [12]. Four MCP-PMTs were made available for this study [1]. All the devices have an 18 mm diameter and 1.2 mm thick optical window, made of borosilicate glass coated with multialkali photocathode, which provides a peak quantum efficiency of about 15% at 500 nm. The amplification stage consists of two stacked layers of 0.4 mm thick MCP wafers made of lead glass, with channel diameters ranging between 7 and 10 μm, and channel pitch ranging between 10 and 12 μm, depending on the device. The channels in the first and second MCP layer have a bias angle to the photodetector axis of 5^o and 13^o, respectively. The photocathode

[1] Courtesy of M. Barnyakov

is separated from the input stage of the MCP by a gap of 0.2 mm, while the gap from the MCP output to the anode is of 0.4 mm.

In addition, we use also one Photonis-XP85012 PMT-MCP, comprising an optical window 53x53 mm^2 wide, and an amplification stage made of two lead glass MCP layers - each 1 mm thick - with 25 μm diameter channels. The optical window, 3 mm thick, is coated with bialkali photocathode providing a peak quantum efficiency of about 22% at 380 nm. The anode readout plane is segmented in 64 pads. In our measurements, this granularity was not exploited, and a common signal (of positive polarity) at the output of the second MCP was read out. This configuration is not optimized for time measurements, as the capacitance associated with the wide readout area impacts on the time response. Therefore, data from these measurements are not exploited to qualify the time performance of Photonis-XP85012, but only to study the secondary emission from the MCPs. Noteworthy, the geometry of the MCP wafers is different from Ekran FEP devices, but the ratio of the channel diameter to the wafer thickness (known as 'aspect ratio') is about 1:40 in both cases. The bias angle is also similar.

A voltage divider is used to provide about 90% of the voltage drop through the MCP layers. Two alternate configurations are used to characterize the MCP response. In the 'PMT-MCP mode', 10% of the voltage drop is equally shared between the photocathode-to-MCP and MCP-to-anode gaps. In this configuration, the response of the detector is driven by avalanches in the MCPs triggered by photoelectrons following Cherenkov emission in the optical window. We estimate that a relativistic particle crossing the optical window at normal incidence generate about four photoelectrons on average. In the 'i-MCP mode', a retarding bias is instead applied to the photocathode-to-MCP gap, to prevent photoelectrons from reaching the MCP surface and triggering an avalanche. In this configuration, the response of the detector is uniquely determined by secondary emission of electrons from the MCP layers when crossed by ionizing particles.

3 Time measurements with cosmic-ray muons

The time response of the Ekran FEP MCPs to single particles was carried out with cosmic-ray muons. The cosmic-ray stand consists of a stack of three MCPs aligned to the vertical. The upper and lower detectors are Ekran FEP MCP photomultipliers, operated in PMT-MCP mode to provide trigger and a reference time measurement, upon the passage of a cosmic ray. The third MCP detector, interposed between the other two, is used either in PMT-MCP or in i-MCP mode. In this setup, the rate of muons within the acceptance of the trigger is about 1 h^{-1}.

Anode signals, with rise time of order 1 ns, are delayed by about 10 ns relative to the trigger, and sampled on a 50 Ω load with a Tektronix DPO7254, providing an 8-bit digitization of the waveforms at 20 GSample/s with an input bandwidth of 2.5 GHz. On each trigger, fired by the coincidence of the upper and lower PMT-MCPs, the waveforms of all the three detectors are recorded for offline analysis. The time information is extracted from interpolated waveforms via constant fraction discrimination (CFD), with a threshold set at 40% of the maximum amplitude. A time-over-threshold algorithm was also tested, and provided comparable performance. Signals are retained in the analysis, if their amplitude is five times larger than the RMS of the electronic noise.

The distribution of the time difference between the MCP detector and one of the MCP trigger signals is shown in Fig.1 for an operating voltage of 2500 V. In the left panel, results are obtained when both detectors are operated in PMT-MCP mode, while in the right panel one of the detectors is operated in i-MCP mode. A time spread of 40 ps is observed in the first case, corresponding to a time resolution of 30 ps to relativistic charged particles in each detector. In the second configuration, the observed time spread is 60 ps, implying that the time resolution of the i-MCP detector to single particles is about 50 ps. While in PMT-MCP mode the detectors are fully efficient to relativistic charged particles, in the i-MCP mode the efficiency ranges between 10% and 50%, depending on the bias voltage. Higher resolution and efficiency are expected for showers, where the multiplicity of secondary particle crossing the MCPs is higher.

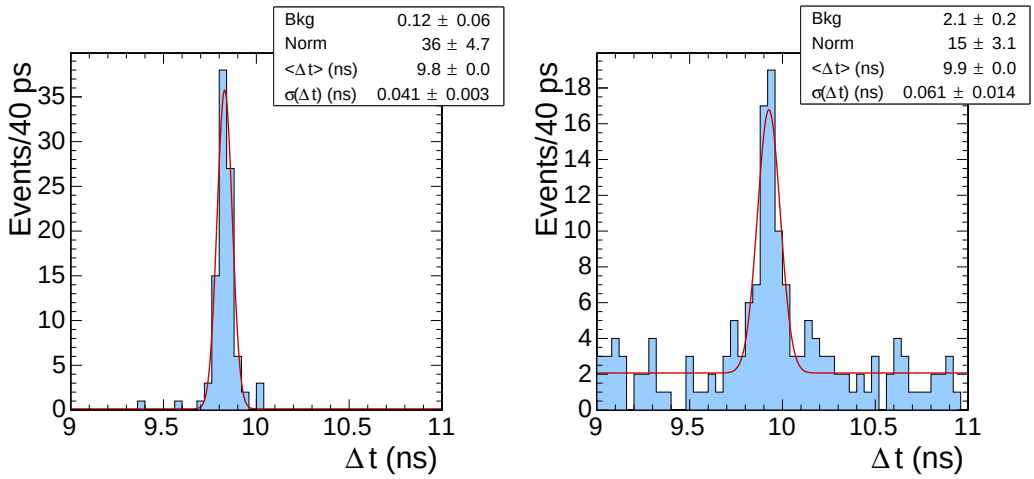

Fig. 1. Distribution of the time difference between signals due to cosmic ray muons through two PMT-MCPs, for signals generated by photoelectrons from Cherenkov emission in the optical window of the two PMT-MCPs (*left*), and for signals generated by secondary emission of electrons at the MCP surface in one of the two PMT-MCPs (*right*).

4 Measurements with 491 MeV electrons

4.1 Setup at the LNF-BTF electron beam

For further characterization of the response and measurement of the efficiency to single particles and to showers, the MCP detectors were exposed to an electron beam at the Beam Test Facility (BTF) of the INFN Laboratori Nazionali di Frascati (Italy) [13]. The beam provides 10 ns long electron pulses with tuneable energy (up to about 500 MeV), repetition rate (up to 49 Hz) and intensity ($1 \div 10^{10}$ particles/pulse). Our measurements were performed with 491 MeV electrons and an intensity tuned to provide a mean multiplicity of about one electron per pulse.

The MCP photomultipliers were mounted in a light-tight box with the optical window towards the beam and orthogonal to the beam direction. The first and last MCPs along the beam line were operated in PMT-MCP mode, to provide a reference event selection for efficiency measurements. A logic signal, synchronous with the beam gate, was used to trigger the waveform digitization of the anode signals, over 200 ns, into a 12-bit 5 GSample/s switched capacitor digitizer (CAEN-V1742). Delays were set to sample about 50 ns of baseline before the signal pulse. Auxiliary beam counters upstream of the MCPs were also readout into gated-ADCs for beam diagnostics and off-line selection purposes. These include a 5 mm thick plastic scintillator with 24×24 mm^2 cross section and a scintillating fibre hodoscope, covering an acceptance of 8×8 mm^2 with 1 mm pitch in the two coordinates transverse to the beam. Further details on this ancillary instrumentation are given in Ref. [14].

Pulses consistent with a single electron entering the test setup, identified from the pulse-height of the signal in the scintillator beam counter, are retained in the offline analysis. Furthermore, the fibre hodoscope is used to identify electrons within the geometric acceptance of the MCPs. The selection is further refined by requesting a pulse in the first PMT-MCP in the beam line, operated in PMT-MCP mode. The charge and the time of each pulse in the downstream MCPs are extracted upon integration and CFD discrimination of the individual waveforms in a time window of 4 ns in coincidence with the signal of the first PMT-MCP. Events are selected if the charge is five times the RMS noise of the detector, measured from the integration of a 4 ns window in the baseline region before the pulse. Empty beam pulses, i.e. with a signal in the scintillator counter consistent with the pedestal, are used to estimate the rate of accidental signals in the MCPs.

4.2 Response to single particles

To measure the efficiency to single electrons, a coincidence is required between the first and the last PMT-MCP along the beam line. Events in the MCP detector under study are accepted if a signal with charge exceeding five times the RMS noise is found in coincidence within 1 ns of the mean time of the reference PMT-MCP signals. The raw efficiency result is corrected for random coincidences of accidental signals falling within the same time window, which amount to less than 0.1% of the triggers.

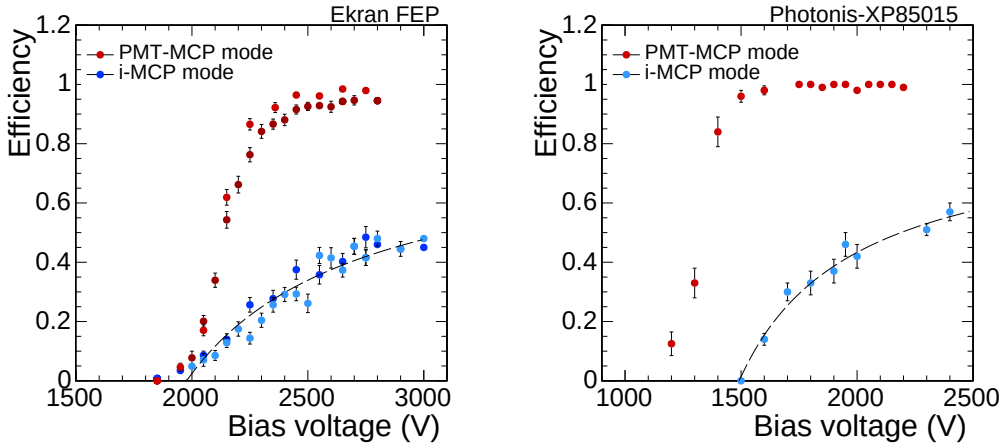

Fig. 2. Efficiency to 491 MeV electrons as a function of the bias voltage for MCP detectors with direct (red dots) and retarding bias (blue dots) between the photocathode and the first MCP layer. The curve through the points is a fit to data of a response model (see text for details). The left panel is for two Ekran FEP MCP detectors; the right panel for Photonis-XP85012.

The efficiencies to 491 MeV electrons as a function of the bias voltage are shown in Fig. 2. Data in the left panel were collected with Ekran FEP MCP photomultipliers operated in PMT-MCP mode (red dots) and in i-MCP mode (blue dots). Results in the right panel refer to Photonis-XP85012: due to limited beam time availability, they include data collected at the cosmic muon test stand.

In PMT-MCP mode, with direct bias to the photocathode, a plateau efficiency close to 100% is achieved with all the devices. In this configuration, secondary emission and amplification are operated by separated elements of the detector: photoelectrons extracted from the photocathode upon Cherenkov emission are amplified above detection threshold by the MCPs. From the properties of the optical window and of the photocathode, we estimate the mean number of photoelectrons to be $\mu \simeq 3 \div 4$ and $15 \div 20$ for the Ekran FEP and the Photonis-XP85012 photodetectors, respectively. Data are well consistent with a residual inefficiency of $\exp(-\mu)$ at plateau, where the MCP gain is sufficient to supply

single photoelectron detection.

In i-MCP mode, a steady increase of the efficiency with the bias voltage is observed above a threshold voltage not lower than in PMT-MCP mode. A maximum efficiency in slight excess of 50% is achieved at the maximum high voltage operated during the tests, but the curve is still not plateauing. In this configuration, the MCP layers carry out the dual function of seeding the cascade process, via the secondary electrons extracted from the MCP, and of providing signal amplification. The amplification process takes place over different channel lengths, depending on the longitudinal position in the channel where the secondary electron is extracted. Inefficiency could arise either because of lack of secondary emission or because of insufficient amplification in the cascade following the secondary emission. The efficiency can therefore be written as:

$$\epsilon = s\left(1 - \frac{L_{eff}}{L}\right), \qquad (L_{eff} \leq L) \tag{1}$$

where s (bound to $s \leq 1$) indicates the probability of secondary emission over the entire MPC length L, and $L_{eff} = L_{eff}(V)$ is the minimum channel length that, at given voltage, provides sufficient gain to overcome the detection threshold. In other words, up to gain fluctuations, secondary emissions in the downstream section of the channel of length L_{eff} do not result in detectable signals; secondary emissions from the complementary section of length $(L_{eff} - L)$ generate detectable signals. Under the hypothesis that the gain over the entire channel has a power-law dependence on the bias voltage, with power index proportional to L, Eq. (1) can be cast in the form:

$$\epsilon = s\left(1 - \frac{1}{b\ln(V/V_{th}) + 1}\right), \qquad (V \geq V_{th}) \tag{2}$$

where V_{th} and b are parameters to be extracted from data. At the threshold voltage V_{th}, secondary electrons generated at the upper surface of the MCP receive just the exact gain to become detectable. Noteworthy, this threshold voltage corresponds to the threshold for single photoelectron detection in PMT-MCP mode: at $V < V_{th}$ the channel length that would be needed to supply sufficient gain for a single photoelectron to be detected would exceed the physical length of the channel ($L_{eff} > L$). In agreement with this, the threshold voltage is approximately the same in both operation modes with the Ekran FEP detectors (Fig. 2-left), for which the mean number of photoelectrons following Cherenkov emission is just slightly above unity. In the Photonis-XP85012 detector with $\mu \simeq 15 - 20$, the efficiency threshold in PMT-MCP mode occurs at an MPC gain that is about one order of magnitude lower than in i-MCP mode, i.e. at a bias voltage about 200 V lower than V_{th} (Fig. 2-right).

The dashed curves in Fig.. 2 show the results of the fit to the data of the model described by Eq.(2). Consistency with data is found for $s \simeq 1$, implying that there is at least one secondary emission following the passage of an ionizing particle through the two MCP wafers. This means that the secondary emission probability from a single wafer is at least 50%. From the aspect ratio and the bias angle of the MCPs, similar in all the devices under study, we estimate that beam electrons at normal incidence on the MCP detectors cross an MCP surface about 10 times as they go through one wafer. We conclude that the secondary emission probability is of order 10% per crossing of a channel surface by the primary particle.

The dependence of the efficiency on the bias voltage is logarithmic, and the efficiency gain on the bias voltage too slow to be practical. Moreover, the signal amplitude depends on where the secondary emission occurs, which may be sub-optimal for some applications. Lines of investigations that we are pursuing to enhance the response to single particles in i-MCP include configurations with multiple MCP stacks, larger bias angles, and wafers with enhanced secondary emission. These variations in assembly or in properties of the wafers impact on the total amount of secondary emission and on the channel gain. Based on our results, for example, we expect that a stack of three MCP wafers could provide an efficiency of 70% or more.

While work is ongoing to refine the MCPs parameters, an efficiency of 50% to single particles looks already promising for applications in environments where the track multiplicity is high. This may be sufficient, for example, to estimate the time of a collision vertex or of electromagnetic showers.

4.3 Response to electromagnetic showers

Further insight in the response of i-MCP detectors is acquired from the analysis of data collected with a set of absorbers of variable thickness in front of the MCP detector under test. Similarly to the previous analysis, trigger counters and one PMT-MCP detector located just upstream of the absorbers are used to identify beam pulses with single electrons entering the test setup. No requirements are instead placed on MCPs downstream of the one under test, not to bias the selected sample with showers with multiplicity of secondary particles higher than the average. Signals in the i-MCP detector exceeding five times the RMS noise and in coincidence with the PMT-MCP within 1 ns are searched for. The efficiency is measured by counting the fraction of these events within the selected sample.

The efficiency to 491 MeV electrons as a function of the absorber thickness, in radiation lengths (X_0) for an i-MCP operating voltage of 2900 V are shown

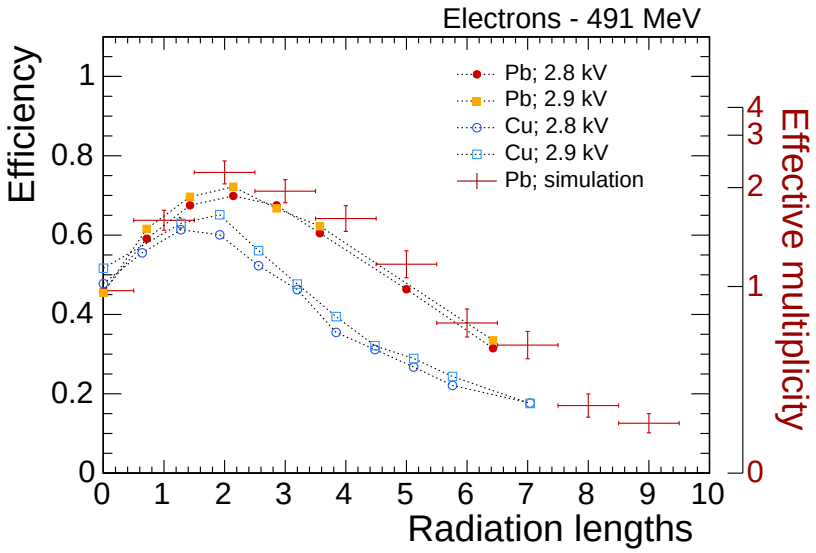

Fig. 3. Efficiency to 491 MeV single electrons in an i-MCP detector as a function of the thickness of lead (full symbols) and copper (open symbols) absorbers. A comparison to simulation for lead (crosses), and the effective multiplicity of particles crossing the MCPs are also shown (see text for details). Errors on the data points are smaller than the marker size. Lines are drawn to guide the eye.

in Fig. 3. Results for two different materials, copper and lead, are displayed. Since lead has a lower critical energy, the multiplicity of secondary particles is expected to be larger with lead absorbers than with copper ones. The efficiency at zero thickness is consistent with the efficiency measured in the analysis of the response to single electrons. As the thickness increases, the efficiency raises from 45% to a maximum of about 70% with the lead absorber at a depth of about $2X_0$. A maximum at a somewhat shallower depth, and with an efficiency of about 65% is observed with a copper absorber. At larger thicknesses, the efficiency decreases and eventually vanishes. This is understood as the effect of the evolution of charged particle multiplicity within the shower for 491 MeV electrons.

Data are also compared to a Monte Carlo (MC) simulation based on the Geant4 package [15, 16]. Electrons of 491 MeV are fired on the absorber. The beam profile is tuned to match the distribution measured at the hodoscope with the events selected by the analysis. Secondary particles from the shower cascade are traced to the MCP surface, and each charged particle with sufficient energy to cross the full thickness of the wafers is assigned a probability $\epsilon = 45\%$ to generate a detectable signal. Primary electrons are counted, if at least one secondary electron generated a signal. This is equivalent to describe the MCP response with a binomial per-event probability:

$$\epsilon(n) = 1 - (1 - \epsilon_0)^n, \tag{3}$$

where ϵ_0 is the efficiency to single particles without absorber, and n is the multiplicity of charged particles crossing the MCP at a given absorber depth. These equation could be used to extract from data the effective multiplicity at each depth. Results from simulation, shown for the lead absorber in Fig.3, are in good agreement with data and confirm our interpretation of the evolution of the response as a function of the absorber depth. According to this interpretation, the efficiency at the maximum corresponds to an effective multiplicity of two charged particles per 491 MeV electron. A multiplicity in excess of four would bring the efficiency to electromagnetic showers above 90%, for $\epsilon_0 = 45\%$. Improvements to the efficiency to single particles in future devices would directly reflect in an improved response to showers.

5 Extrapolation to photons of high energy

The simulation and the response model are extended to evaluate the potential of photon timing at high energies with MCP detectors embedded in a preshower. A detailed design study is beyond the scope of this document, but we focus on two aspects to help clarify some performance requirements: on the one side, precision timing could be fully exploited if achieved with sufficient efficiency, and on the other, the impact on the energy resolution of the calorimeter system should remain small. Both aspects are studied in dedicated simulations.

In the study of the efficiency, electrons and photons of 30 GeV are simulated and propagated through the same MC simulation shown to match test beam results (see Sec. 4). These energies are representative of physics processes relevant at the HL-LHC. We find that one i-MCP detector with 45% efficiency to single particles would be sufficient to provide full efficiency to electrons and more than 80% efficiency for photons after $3X_0$ of lead. The increase in efficiency relative to direct measurements with 491 MeV electrons should be ascribed to the higher multiplicity of secondary particles in 30 GeV showers. The efficiency to photons would rise to above 90%, with two sampling layers at $1X_0$ and $3X_0$, or alternatively with a single layer, if the efficiency to single particles could be increased to 70%. The difference in efficiency between electrons and photons reflects the conversion probability of photons in the absorber. At full MCP efficiency, a residual, irreducible inefficiency of approximately 5% to photons in a $3X_0$ preshower would still be observed. As we commented earlier, work is ongoing to enhance the single particle efficiency.

To study the impact on the energy resolution, the simulation, used so far only to count particles below the detection threshold, is extended to include the analog response of i-MCPs. In i-MPC mode, the gain of the detector depends on the position along the MCP channel where the secondary emission occurs.

As a consequence, the amplitude spectrum observed with single particles at the test beam is broad and approximately flat above the threshold amplitude up to a maximum amplitude. This is implemented in simulation by randomly sampling a uniform distribution for $\epsilon = 45\%$ of the particles crossing the MCP detectors, randomly selected, and ascribing zero amplitude to the remaining particles. Even if the single particle response is broad, the mean response is still proportional to particle multiplicity crossing the i-MCP and, in turn, to the energy deposited in the $3X_0$ absorber. This relationship defines the amplitude to energy calibration of the MC simulation. After calibration, events are generated scanning several energies from 10 to 300 GeV. The energy deposited in the preshower in each event is estimated from the amplitude and added to the energy deposited in a calorimeter block downstream of the preshower, with ideal resolution. With this procedure, the resulting energy sum is only smeared by the amplitude response spread due to the preshower, and is therefore suited to predict the resolution term that this preshower would add to the calorimeter. According to simulation, we find this contribution to be smaller than $5\%/\sqrt{E(\mathrm{GeV})}$, which is definitely a small contribution for most electromagnetic calorimeters.

6 Summary and outlook

We report on the response of microchannel plates (MCPs) to single relativistic particles and to electromagnetic showers. Several prototypes of photodetectors with the amplification stage based on MCPs were exposed to cosmic rays and to 491 MeV electrons at the INFN-LNF Beam-Test Facility. The MCPs were used as secondary emission detectors, by applying a retarding bias to the photocathode. In this configuration, time resolutions of about 50 ps with cosmic muons, and detection efficiencies to single relativistic particles of order 50% are obtained. Measurement with electromagnetic showers sampled at different depths shows that the MCPs efficiency has a simple binomial dependence on the multiplicity of particles in the shower. Starting from the interpretation of the results, lines of investigations to further enhance the response of detectors relying on secondary emission from the MCP surface are suggested. While these investigations are being pursued, we show that present results make this detection technique worth considering for application in the precision timing of high energy photons and charged particles, to aid in event reconstruction at high luminosity colliders.

Acknowledgements

We gratefully acknowledge the skilful help and continuous support of R. Bertoni, R. Mazza, M. Nuccetelli and F. Pellegrino for the preparation of the experimental setup. We are indebted to B. Buonomo, L. Foggetta and P. Valente for their help with the setup of the beam facility. We also thank our students A. Beschi, S. Bologna, M. Defranchis and M. Gregori for valuable contributions. This work is supported by INFN CSN5.

References

[1] M. Abbrescia et al. ECFA High Luminosity LHC Experiments Workshop: Physics and Technology Developments Summary submitted to ECFA. 96th Plenary ECFA meeting. Jan 2015.

[2] Sebastian N. White. R&D for a Dedicated Fast Timing Layer in the CMS Endcap Upgrade. *Acta Phys. Pol. B Proc. Suppl.*, 7:743, 2014.

[3] Betty Bezverkhny Abelev et al. Performance of the ALICE Experiment at the CERN LHC. *Int.J.Mod.Phys.*, A29:1430044, 2014.

[4] Georges Aad et al. Search for nonpointing and delayed photons in the diphoton and missing transverse momentum final state in 8 TeV *pp* collisions at the LHC using the ATLAS detector. *Phys.Rev.*, D90(11):112005, 2014.

[5] Daniele Del Re. Timing performance of the CMS ECAL and prospects for the future. *Journal of Physics: Conference Series*, 587(1):012003, 2015.

[6] J. L. Wiza. Microchannel plate detectors. *Nucl.Instrum.Meth.*, 162:587, 1979.

[7] A.A. Derevshchikov, V. Yu. Khodyrev, V.I. Kryshkin, V.E. Rakhmatov, and A.I. Ronzhin. On possibility to make a new type of calorimeter: Radiation resistant and fast. *Report, IFVE-90-99, Protvino*, 1990.

[8] M. Bondila, L. Efimov, D. Hatzifotiadou, G. Feofilov, V. Kondratev, et al. Results of in-beam tests of an MCP-based vacuum sector prototype of the T0/centrality detector for ALICE. *Nucl.Instrum.Meth.*, A478:220–224, 2002.

[9] Bernhard Adams, Andrey Elagin, Henry Frisch, Razib Obaid, Eric Oberla, et al. Measurements of the gain, time resolution, and spatial resolution of a 20x20cm^2 MCP-based picosecond photo-detector. *Nucl.Instrum.Meth.*, A732:392–396, 2013.

[10] A. Ronzhin, S. Los, E. Ramberg, M. Spiropulu, A. Apresyan, et al. Development of a new fast shower maximum detector based on microchannel plates photomultipliers (MCP-PMT) as an active element. *Nucl.Instrum.Meth.*, A759:65–73, 2014.

[11] A. Lehmann, A. Britting, W. Eyrich, F. Uhlig, R. Dzhygadlo, et al.

Improved lifetime of microchannel-plate PMTs. *Nucl.Instrum.Meth.*, A766:138–144, 2014.

[12] A. Yu. Barnyakov, M. Yu. Barnyakov, V.S. Bobrovnikov, A.R. Buzykaev, S.A. Kononov, et al. Investigation and development of microchannel plate phototubes. *Nucl.Instrum.Meth.*, A572:404–407, 2007.

[13] A. Ghigo, G. Mazzitelli, F. Sannibale, P. Valente, and G. Vignola. Commissioning of the DAFNE beam test facility. *Nucl.Instrum.Meth.*, A515:524–542, 2003.

[14] Vieri Candelise et al. Beam test results for a tungsten-cerium fluoride sampling calorimeter with wavelength-shifting fiber readout. *Proc. IEEE Nuclear Science Symposium*, paper N17.6, 2014.

[15] M. Asai. Geant4-a simulation toolkit. *Trans.Amer.Nucl.Soc.*, 95:757, 2006.

[16] John Allison, K. Amako, J. Apostolakis, H. Araujo, P.A. Dubois, et al. Geant4 developments and applications. *IEEE Trans.Nucl.Sci.*, 53:270, 2006.